Mechanism of DNP-Enhanced Polarization Transfer across the Interface of Polycarbonate/Polystyrene Heterogeneous Blends

Mobae Afeworki† and Jacob Schaefer*

Department of Chemistry, Washington University, St. Louis, Missouri 63130

Received November 13, 1991

ABSTRACT: In DNP difference experiments, the same integrated intensity is observed for the interface-PC signal in PC(^{13}C)/PS(^{12}C/*) and PC(^{13}C)/PS(^{2}D/*) thin-film blends (see previous paper for sample notation). This result proves that the dominant mechanism of polarization transfer from the electrons in the PS phase to the protons in the PC phase is by direct polarization transfer. The interface-PC signal intensity arises from a 60-Å region which is 2% of the PC film thickness. Minor polarization transfer from the DNP-enhanced protons of PS to the PC protons across the PC/PS interface via H–H spin diffusion in PC(^{13}C)/PS(^{12}C/*) may also occur. Even in BDPA-doped homopolymers, the enhancement mechanism is mainly via direct solid-effect polarization transfer, a conclusion based on the similarity of the time dependence of the electron–proton polarization transfers for PS(*) and PS(^{2}D/*).

Introduction

The DNP-enhanced PC-interface signal of Figure 12 (top, δ_C 120) of the previous paper (part 1) was obtained by a double-polarization transfer: electrons to protons to carbons. In this paper, we report the time dependence of the first transfer, electrons to protons, and discuss whether this solid-effect transfer is from electrons to PS protons or from electrons to PC protons.

Time Dependence of the Solid-Effect Transfer

For irradiation at the difference of the electron and proton Larmor frequencies, the time dependence of the positive DNP enhancement of proton polarization is described by

$$\frac{dP_I}{dt} = -N_S W(P_I - P_S) - \frac{1}{T_I}(P_I - P_I^0) \quad (1)$$

$$\frac{dP_S}{dt} = -N_I W(P_S - P_I) - \frac{1}{T_S}(P_S - P_S^0) \quad (2)$$

These are eqs 10 and 11 in part 1, where definition of the terms may be found. Under most experimental conditions pumping of microwave transitions is slow and the rate of change of the electron Zeeman population is small compared to that of the proton Zeeman population. Thus

$$dP_S/dt = 0 \quad (3)$$

$$P_S = \frac{P_I + P_S^0/N_I T_S W}{1 + 1/N_I T_S W} \quad (4)$$

Substitution of eq 4 into eq 1 and subsequent integration leads to

$$P_I = \frac{1}{A}[B - C\exp(-At)] \quad (5)$$

where

$$A = ac + b \quad (6)$$

$$B = acP_S^0 + bP_I^0 \quad (7)$$

$$C = B - AP_I^0 \quad (8)$$

$$a = \frac{1}{T_S(1 + 1/N_I T_S W)} \quad (9)$$

$$b = 1/T_I \quad (10)$$

$$c = N_S/N_I \quad (11)$$

Thus, P_I is P_I^0 at the start of the microwave irradiation when $t = 0$ and then approaches the DNP enhancement of B/A (which is also given by eq 13, part 1) exponentially in time with a rate constant, A. Equations 6 and 9–11 show that in principle, this *microscopic* rate constant is always greater than T_I^{-1}. However, in practice sometimes the initial rate of growth of the observed DNP enhancement appears to be less than T_I^{-1}. This occurs because many of the protons that are coupled to electrons and involved in the solid-effect transfer are frequency shifted from other protons. The frequency-shifted protons are not part of the detected signal and have their own T_I's which are longer than the bulk T_I. (A specific example is described in part 4.) The observed *macroscopic* growth rate is therefore a composite process that involves electron–proton polarization transfer via H–H spin diffusion to nearby protons less tightly coupled to the electron and more easily detected. The *net* growth rate includes additional spin diffusion to all other more remote protons in the sample. These two diffusion processes are distinct; the first is between protons whose resonance frequencies are mismatched, while the second is between protons whose resonance frequencies are matched. In the following section, we describe the first process phenomenologically and the second process as Fickian diffusion.

One-Dimensional Fickian Diffusion with Spin–Lattice Relaxation from a Point Source of Magnetization

We model the transfer of DNP-enhanced polarization to remote, frequency-matched protons as one-dimensional Fickian diffusion with spin–lattice relaxation (Figure 1). Protons contributing to the source of magnetization are

† Present address: Exxon Research and Engineering Co., Annandale, NJ 08801.

0024-9297/92/2225-4092$03.00/0

near the free-radical center. For computational purposes, we replace the standard differential equation involving the diffusivity constant, D

$$\frac{\partial u(t,x)}{\partial t} = D\frac{\partial^2 u(t,x)}{\partial x^2} \tag{12}$$

with a difference equation[1]

$$\frac{1}{h}(u_{i,j} - u_{i-1,j}) = \frac{D}{k^2}(u_{i-1,j+1} - 2u_{i-1,j} + u_{i-1,j-1}) \tag{13}$$

in which h and k scale the size of the time and space steps, and i and j are the difference-equation time and space variables, respectively. We add spin–lattice relaxation to obtain

$$\begin{aligned} u_{i,j} = u_{i-1,j} + \lambda\{&[D(x_j + k/2)][u_{i-1,j+1} - u_{i-1,j}] - \\ &[D(x_{j-1} + k/2)][u_{i-1,j} - u_{i-1,j-1}] - \\ &[1 - \exp(-(i-1)h/T_1(x_j + k/2))][u_{i-1,j}]\} \end{aligned} \tag{14}$$

Because polarization can cross the PC/PS interface, the diffusivity D and the proton spin–lattice relaxation time T_1 depend on position in eq 14. That is

$$D = D(x_j)$$

$$T_1 = T_1(x_j) \tag{15}$$

If there are T time steps of size h, and X space steps of size k, then

$$i = 1, 2, 3, ..., T$$

$$j = 1, 2, 3, ..., X \tag{16}$$

$$x_j = jk \tag{17}$$

The scaling ratio in eq 14 is given by λ where

$$\lambda = h/k^2 \tag{18}$$

The boundary conditions reflect the macroscopic growth of (normalized) DNP-enhanced polarization

$$u_{i,0} = [1 - \exp(-\alpha ih)] \tag{19}$$

$$u_{0,j} = 0 \tag{20}$$

Equation 19 has the same form as eq 5; thus, α is a phenomenological rate constant that describes the composite process of solid-effect transfer from electrons to protons, plus H–H spin diffusion between protons with mismatched Larmor frequenices.

The diffusion eq 14, with the boundary conditions given by eqs 19 and 20, was solved numerically on a microcomputer. The solution was obtained with $T = 100$, $X = 20$, and the diffusivities and spin–lattice relaxation times of Table I. A value of 1.5 s^{-1} was chosen for α in eq 19. This rate matches the growth in the DNP enhancement for the residual protons in PC(^{13}C)/PS(^{2}D/*) (part 1). On the basis of the τ_c's (time constants for H–H spin exchange) and D's of Table I, each increment in x_j (eq 17) represents 30 Å. Polystyrene has a density of 1.05 g cm^{-3}. Taking 15 Å as an approximate linear dimension for BDPA means that for 2% doping by weight, the average distance between uniformly dispersed free-radical centers is approximately 70 Å. Calculated polarization concentration profiles are shown in Figure 2. The top row shows the polarization concentration gradient in PS, and the bottom row, the gradient in PC. The calculation assumed changes in D's and T_1's from PS to PC values, two steps or 60 Å from the BDPA source of polarization in the PS phase.

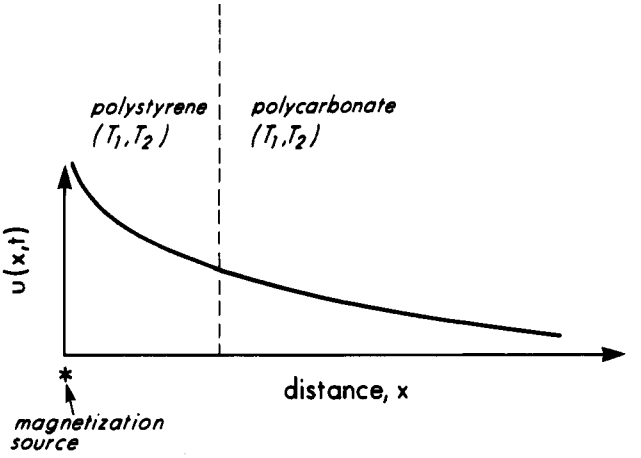

Figure 1. Hypothetical polarization gradient resulting from H–H spin diffusion away from a source of DNP-enhanced magnetization in a free-radical doped polymer with variable ^{1}H T_1's and T_2's. The source of magnetization is protons near the free-radical centers but with resonance frequencies matched to that of the bulk protons. The dotted line indicates a compositional change in the medium such as that which occurs at the interface between PC and PS in thin-film heterogeneous blends.

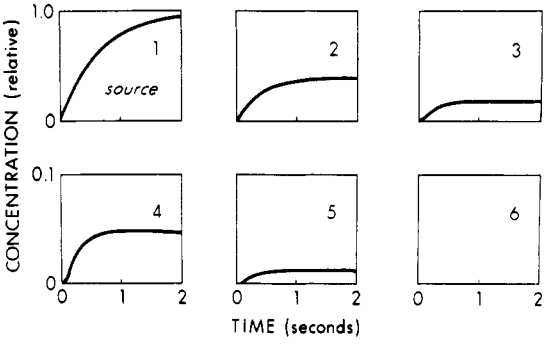

Figure 2. Calculated concentration profiles resulting from frequency-matched H–H spin diffusion with spin–lattice relaxation (panels 2–6) away from a source of magnetization (panel 1). The calculation is the solution to eq 14 with the boundary conditions of eq 19 and 20, the parameters of Table I, and α = 1.5 s^{-1}. The top row represents the polarization gradient in BDPA-doped PS, and the bottom row, the polarization gradient in the BDPA-free PC in a heterogeneous thin-film blend. Each panel represents a 30-Å step away from the magnetization source which is protons polarized by a direct solid-effect transfer from electrons. The PC/PS interface is 60 Å from the magnetization source.

Table I
Parameters for Fickian Diffusion Calculations

	polystyrene	polycarbonate
H_L, kHz[a]	8	4
τ_C(1.5 Å), ms[b]	0.04	0.08
$1/\tau_C$(30 Å), s^{-1} [c]	50	25
D, 10^{-12} cm^2/s[d]	4.50	2.25
T_1(H), s[e]	1	0.1

[a] From experiment, ref 3. Molecular motion reduces H_L in PC. [b] From $\tau_C = 1/\pi H_L$, assuming an average interproton distance of 1.5 Å. [c] From τ_C(30 Å) = 400τ_C(1.5 Å). [d] From $D = \langle x\rangle^2/\tau_C$. [e] From experiment, this work.

Experiments

BDPA-Doped PS and Perdeuterated PS. The BDPA-doped PS is the sample described in part 1. Perdeuterated styrene, 98% styrene-d_8, was purchased from Merck Stable Isotopes (Montreal, Canada) and was thermally polymerized to PS. The BDPA-doped perdeuterated PS sample, PS(^{2}D/*), was prepared in the same way as the BDPA-doped PS (part 1). DNP

enhancements for doped homopolymers were measured using a $90_y-\tau-90_x-\tau$ ^1H solid echo.

Thin-Film Blends. A thin-film blend of ^{13}C-enriched PC and BDPA-doped 98% perdeuterated PS, denoted as PC(^{13}C)/PS(^2D/*), was prepared in a manner identical to that used to prepare the thin-film blend of ^{13}C-enriched PC and BDPA-doped, ^{13}C-depleted PS. Comparisons were made of the difference spectra of PC(^{13}C)/PS(^2D/*) and PC(^{13}C)/PS(^{12}C/*) obtained using the DNP CPMAS ^{13}C NMR experiment described in part 1. These comparisons were of the results of experiments performed under identical conditions: the spectra were obtained back-to-back using the same microwave power of 5 W and exactly 12 000 scans for each experiment. The CPMAS spectrum of PS(*) was subtracted from the DNP difference spectrum of PC(^{13}C)/PS(^2D/*) to remove the contribution of the residual natural-abundance ^{13}C phenyl-ring carbons of PS(^2D) from the difference signal. The PS(*) spectrum was scaled so that the aliphatic-carbon signal in the PS(^{13}C)/PS(^2D/*) spectrum was matched.

The DNP CPMAS ^{13}C NMR experiment was done on the thin-film blend PC(^{13}C)/PS(^{12}C/*) with microwave-irradiation times varied from 0.4 to 2.0 s. The sequence of the irradiation times was 2.0, 0.4, 1.6, 0.8, 1.2, 0.6, 1.0, 1.8, and 1.4 s, respectively. A total of nine files corresponding to nine different irradiation times, each containing 3000 scans, were collected and the experiment was repeated six times for a total of 18 000 scans for each microwave-irradiation time. In order to avoid a droop in microwave power during the experiment due to aging of the klystron, the microwave power level was intentionally set at a value lower than the maximum available. At the time of this experiment the maximum available power was 4 W, and the experiment was performed at 2.5 W. Doing the experiment at lower power levels had the incidental advantage that the interfacial-PC signals were relatively well resolved, making quantitation easier (part 1, Figure 14).

Results

DNP of Protons in BDPA-Doped PS and Perdeuterated PS. The proton NMR spectra of the residual protons in 98% perdeuterated polystyrene, PS(^2D), obtained by using a standard proton solid-echo experiment, are well enough resolved that aromatic- and aliphatic-proton signals can be distinguished (Figure 3, bottom). Spinning sidebands extending over about ±6 kHz arise from $^1H-^2D$ and residual $^1H-^1H$ inhomogeneous dipolar coupling.[2]

When the perdeuterated PS sample was doped with 2% by weight BDPA, the proton line width (full width at half maximum) increased to 1.3 kHz for the residual protons. The aromatic- and aliphatic-proton resonances are not resolved (Figure 3, top). This broadening is due to dipolar coupling to the unpaired electrons in BDPA ($T_{1e} = 750\ \mu s$). The proton line width of 1.3 kHz is a factor of 20 less than that of the fully protonated PS but a factor of 2 greater than susceptibility broadening. An upper limit for the susceptibility broadening is assessed by the ^{13}C line width in a similarly doped sample (Figure 3, insert).

The positive DNP enhancement observed for PS(*) using the proton solid-echo experiment is a factor of 20 for 10-W microwave power applied for 2 s (part 1). For 5-W microwave power, the DNP enhancement for PS(*) reaches a value of about 10 in 1 s, while that for the residual protons in PS(^2D/*) reaches the same value but requires additional microwave pumping time (Figure 4). The enhancement in PS(^2D/*) has not quite reached a plateau after 2 s of microwave irradiation. The extrapolated, infinite-power enhancement of PS(^2D/*) is about 1.5 times larger than that of PS(*).

DNP of Thin-Film Blends. A comparison of the integrated intensities of the DNP-enhanced interface signal from PC(^{13}C)/PS(^2D/*) and PC(^{13}C)/PS(^{12}C/*) shows that the two thin-film blend samples give rise to about the same PC integrated intensity (Figure 5, top and bottom). The interface-PC signal and the unenhanced, standard CPMAS ^{13}C NMR signal of bulk PC in this particular PC(^{13}C)/PS(^2D/*) thin-film blend are both broadened by an inhomogeneous local susceptibility effect. This result was established from echo intensities in rotor-synchronized, Carr-Purcell refocusing experiments which are described in part 3.

Although, the DNP-enhanced bulk PC ^1H and ^{13}C signal intensities in PC(^{13}C)/PS(^{12}C/*) increase monotonically with microwave pumping, the DNP-enhanced interface PC signal reaches a maximum after about 1.2 s of microwave pumping and then decreases. The DNP CPMAS ^{13}C difference spectra for 0.4-, 1.2-, and 2.0-s microwave irradiation times are shown in Figure 6. The complete dependence of the intensity of the DNP-enhanced PC-interface signal as a function of the micro-

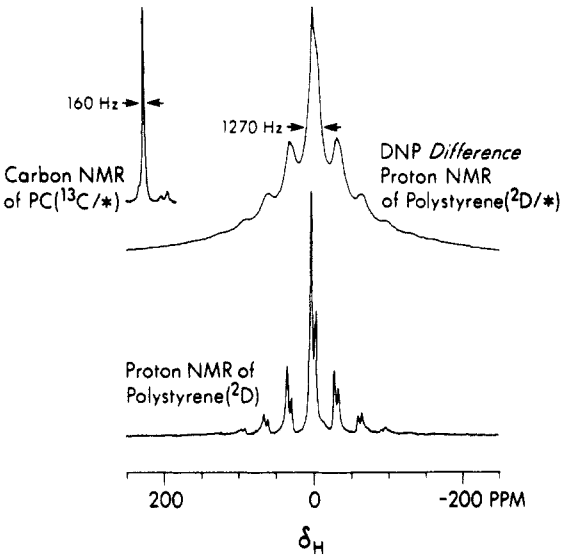

Figure 3. 1.4-T solid-echo ^1H NMR spectrum of the residual protons in 98% perdeuterated PS spinning at the magic angle at 1859 Hz (bottom). Signals from aromatic and aliphatic protons are resolved. Spinning sidebands are due primarily to heterogeneous $^1H-^2D$ and $^1H-^1H$ dipolar coupling. The DNP-enhanced ^1H NMR spectrum from BDPA-doped perdeuterated PS has similar spinning sidebands but is less well resolved (top). A 1.4-T ^{13}C NMR spectrum is shown for comparison in the insert (top left).

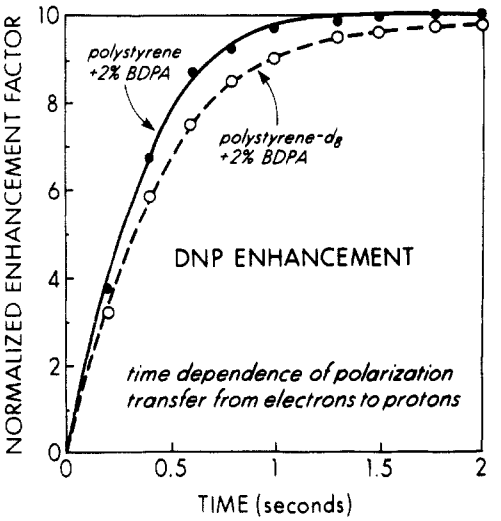

Figure 4. DNP enhancement of the ^1H NMR signal intensity as a function of the microwave-irradiation time for PS(*) and PS(^2D/*).

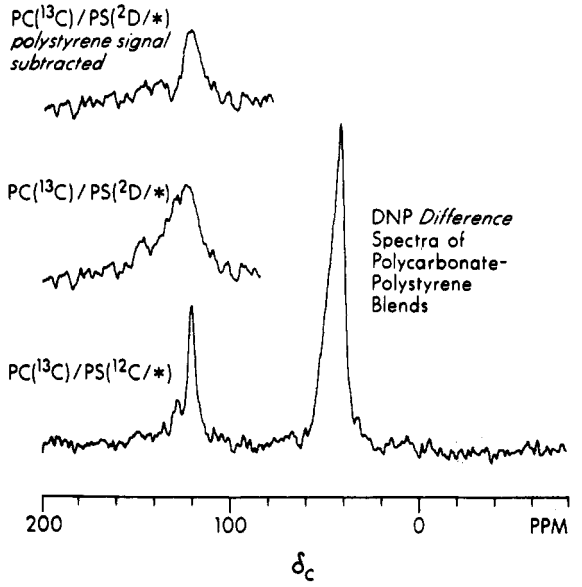

Figure 5. DNP difference ^{13}C NMR spectra of thin-film blends of PC(^{13}C)/PS(^{12}C/*) (bottom) and PC(^{13}C)/PS(^{2}D/*) (top two inserts). The spectrum in the middle insert arises both from natural-abundance carbons coupled to the residual protons in perdeuterated bulk PS and from label in ^{13}C-enriched interface PC.

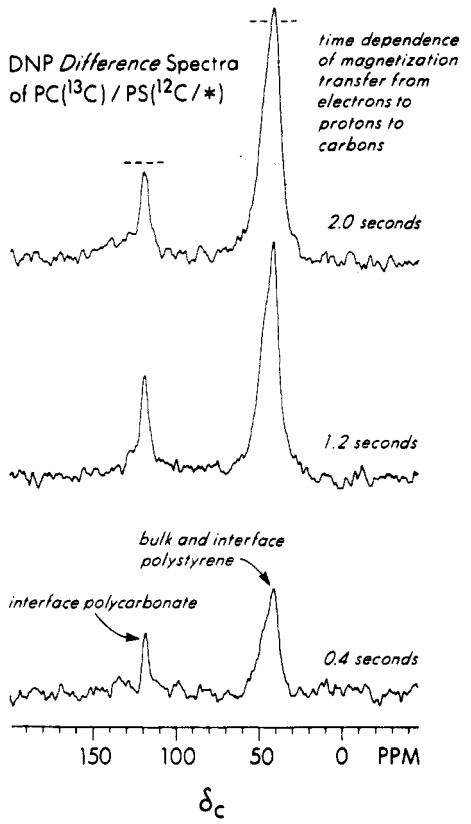

Figure 6. DNP difference ^{13}C NMR spectra of PC(^{13}C)/PS(^{12}C/*) as a function of the microwave-irradiation time. The DNP enhancement for interface PC reaches a maximum after irradiation for about 1.2 s, while that of the bulk PS monotonically increases with the microwave-irradiation time. The horizontal dashed lines indicate signal levels for 1.2-s microwave-irradiation times.

wave irradiation time is shown in Figure 7 (solid circles, right panel).

Discussion

Mechanism of Polarization Transfer in Doped PS and Perdeuterated PS. The dominant transfer mechanism in BDPA-doped polystyrene is a direct electron-to-proton solid-effect enhancement. Proton–proton spin diffusion helps to redistribute polarization but is not essential. Disruption of H–H spin diffusion by deuteration does not reduce the DNP enhancement factor (Figure 4). Because spin diffusion allows polarization to move 50–100 Å in 1 s in fully protonated PS,[2] and because deuteration of PS only slows reaching full DNP enhancement for the residual protons but not the enhancement itself, we conclude that the electron–proton solid effect operates over distances comparable to 50 Å. This conclusion is consistent with the linear dependence of DNP enhancement with microwave power shown in part 1 (Figure 7). With one electron per 2000 protons in fully protonated PS and with electrons separated by less than 100 Å, sizeable DNP enhancements can be generated by direct electron-to-proton polarization transfers even with T_{1e}'s of 1 ms.

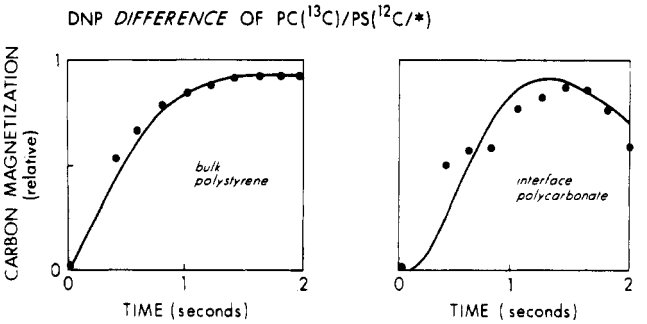

Figure 7. Relative DNP difference ^{13}C NMR signal intensities as a function of microwave-irradiation time for bulk PS (left) and total interface PC in PC(^{13}C)/PS(^{12}C/*). Circles are experimental points. Solid curves were calculated from a Fickian diffusion model (with spin-lattice relaxation) of spin diffusion using the parameters of Figure 9.

Any contribution of spin diffusion to the observed DNP enhancement in PS(^{2}D/*) still involves a slow transfer under frequency-mismatched conditions, from protons directly polarized by a solid-effect transfer to nearby protons. More distant protons are, however, not polarized by the fast spin diffusion illustrated in panels 2 and 3 of Figure 2 but rather are directly polarized by a slower version of the solid-effect composite process represented by panel 1. The resulting distribution of transfer rates explains the absence of a plateau for the DNP enhancement of PS(^{2}D/*) in Figure 4.

Mechanism of Polarization Transfer in PC/PS Thin-Film Blends. The positive proton polarization generated by microwave pumping of PC(^{13}C)/PS(^{12}C/*) at the difference of the electron and proton Larmor frequencies can cross the PC/PS boundary either by H–H dipolar contact between protons of PC and PS and spin diffusion or by direct solid-effect enhancement of PC protons by electrons in the PS phase or by a combination of the two pathways. This situation is illustrated in Figure 8.

Because removal of at least 98% of the protons on the PS side of the PC/PS interface in thin-film blends has no effect on the integrated intensity of the interface-PC signal (Figure 5), the dominant solid-effect transfer is from electrons in the PS phase that are of the order of 50 Å from the interface to protons in the PC phase. On the basis of the PS(^{2}D/*) results discussed above, we know that direct transfers over these distances occur. In fact, we believe that the narrow carbon line width observed for low-power microwave irradiation (Figure 14, part 1) arises because more distant protons avoid frequency-mismatched polarization-transfer bottlenecks and so are the first to be detected.

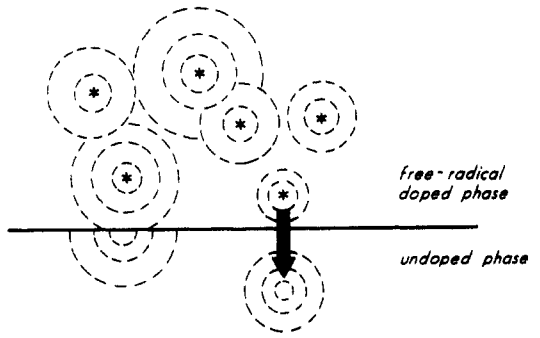

Figure 8. Two modes of polarization transfer (directly or indirectly, the latter by ^1H–^1H spin diffusion) from electrons (stars) to protons in the undoped phase of a two-phase heterogeneous blend.

The DNP-enhanced interface-PC signal intensity is 4% of the unenhanced bulk-PC signal intensity in the thin-film PC(^{13}C)/PS(^{12}C/*) blend. Taking into account the DNP enhancement factor of 2 for PC protons at half microwave power (part 1, Figure 7), the interface-PC signal is qualitatively consistent with a 60-Å-thick interface or about 2% of the 3000-Å-thick PC thin film. In comparing interface-PC signals to bulk-PS signals, the ^{13}C isotopic enrichment of PC at the interface offsets the ratio of interface material to bulk material. Therefore, because the solid-effect enhancement for PS protons is 5 times that of PC protons (part 1), we expect the bulk-PS, aliphatic-carbon signal intensity (δ_C 45) to be about 5 times that of the interface-PC, aromatic-carbon signal (δ_C 120). Experiment shows a ratio of approximately five-to-one (Figure 5, bottom).

We believe that the observed decrease in PC polarization with increasing time of microwave irradiation (Figure 6) is due to a shortening of the PC T_1(H) by local inductive heating. Faster PC spin–lattice relaxation would increase spin–lattice polarization leakage and thus reduce the enhancement. Another explanation involving spin diffusion is offered below.

Spin-Diffusion across the Interface of the PC–Protonated PS Blend. Even though inductive heating is a plausible explanation for the maximum in the interface-PC signal with microwave irradiation, we cannot eliminate spin diffusion as a minor contributor. The results of the calculation of Figure 2 show that polarization originating in the fully protonated PS phase can reach and cross the interface to the PC phase. However, the calculation shows a plateau for PC polarization with increasing time of microwave irradiation rather than the observed decrease (Figure 6). We find that we can account for such a decrease by the calculation only if we reduce D and $T_1(H)^{-1}$ of both PS and PC by a factor of about 100 relative to α (Figure 9). With slower spin diffusion, the effect of relaxation has time to accumulate, thereby altering the shapes of the concentration profiles. As long as we maintain the same ratios of D's to $T_1(H)^{-1}$'s as in Table I, the total PC-interface polarization is comparable to that of the calculation of Figure 2. But now the calculated time dependence of interface polarization in PC matches the observed maximum near $t = 1.5$ s (Figure 7, right). The step size of the difference-equation calculation still corresponds to 30 Å if the time constant for H–H spin exchange, τ_c (Table I), has also increased by a factor of a 100.

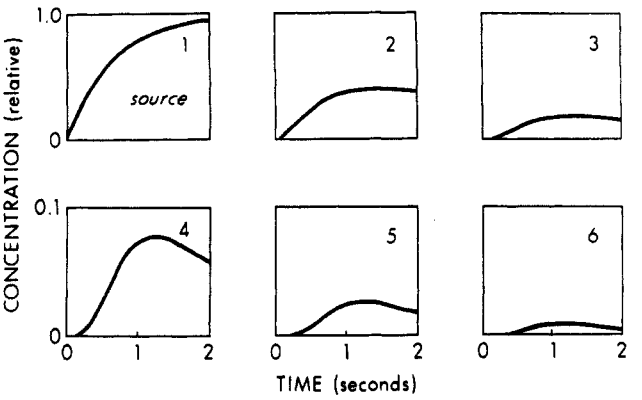

Figure 9. Similar calculated concentration profiles to those described in the caption to Figure 2 but with $D = 9 \times 10^{-14}$ cm^2 s^{-1} and $T_1 = 200$ s for PS (top row), $D = 4.5 \times 10^{-14}$ cm^2 s^{-1} and $T_1 = 40$ s for PC (bottom row), and $\alpha = 1.5$ s^{-1}. The anomalously slow spin diffusion is assumed to result from Larmor-frequency offsets (mismatches) arising from dipolar coupling to free electrons near the interface. Slow spin–lattice relaxation is assumed to result from Zeeman pumping by a local, direct solid-effect DNP enhancement.

We can rationalize the reductions in D's as due to frequency offsets arising from variations in dipolar coupling to free electrons near the interface and those in $T_1(H)^{-1}$'s as due to a balancing of Zeeman relaxation by a direct, long-range solid-effect enhancement. However, adopting this rationalization implies that electron-to-proton transfers are indeed long range and so can cross the PC/PS interface directly without the assistance of spin diffusion.

Acknowledgment. The perdeuterated polystyrene was synthesized by R. J. Kern (Monsanto Co., St Louis). This work has been supported by the Office of Naval Research.

References and Notes

(1) Crank, J. *Mathematics of Diffusion*; Oxford University Press: Oxford, U.K., 1956; Chapter X.
(2) VanderHart, D. L.; Manders, W. F.; Stein, R. S.; Herman, W. *Macromolecules* **1987**, *20*, 1724.
(3) Schaefer, J.; Sefcik, M. D.; Stejskal, E. O.; McKay, R. A. *Macromolecules* **1981**, *14*, 280.

Registry No. PS (homopolymer), 9003-53-6.